Eur. Phys. J. A **18**, 633–638 (2003)
DOI 10.1140/epja/i2002-10165-x

THE EUROPEAN PHYSICAL JOURNAL A

Cross-section limits for the ^{208}Pb(^{86}Kr, n)^{293}118 reaction

K.E. Gregorich[1,a], T.N. Ginter[1], W. Loveland[2], D. Peterson[2], J.B. Patin[1,3], C.M. Folden III[1,3], D.C. Hoffman[1,3], D.M. Lee[1], H. Nitsche[1,3], J.P. Omtvedt[4], L.A. Omtvedt[4], L. Stavsetra[4], R. Sudowe[1], P.A. Wilk[1,3], P.M. Zielinski[1,3], and K. Aleklett[5]

[1] Nuclear Science Division, Lawrence Berkeley National Laboratory, Berkeley, CA 94720, USA
[2] Department of Chemistry, Oregon State University, Corvallis, OR 97331, USA
[3] Department of Chemistry, University of California, Berkeley, CA 94720, USA
[4] University of Oslo, Oslo, Norway
[5] Uppsala University, Uppsala, Sweden

Received: 2 September 2002 / Revised version: 10 April 2003 /
Published online: 18 November 2003 –
Communicated by W. Henning

Abstract. In April-May, 2001, the previously reported experiment to synthesize element 118 using the ^{208}Pb(^{86}Kr,n)^{293}118 reaction was repeated. No events corresponding to the synthesis of element 118 were observed with a total beam dose of 2.6×10^{18} ions. The simple upper-limit cross-sections (1 event) were 0.9 and 0.6 pb for evaporation residue magnetic rigidities of 2.00 Tm and 2.12 Tm, respectively. A more detailed cross-section calculation, accounting for an assumed narrow excitation function, the energy loss of the beam in traversing the target and the uncertainty in the magnetic rigidity of the $Z = 118$ recoils is also presented. Re-analysis of the primary data files from the 1999 experiment showed the reported element 118 events are not in the original data. The current results put constraints on the production cross-section for synthesis of very heavy nuclei in cold-fusion reactions.

PACS. 25.70.Gh Compound nucleus – 25.70.Jj Fusion and fusion-fission reactions – 27.90.+b $220 \leq A$

1 Introduction

In 1999, the synthesis of element 118 (and its decay products) using the ^{208}Pb(^{86}Kr,n) reaction was reported [1]. This claim was based on the apparent occurrence of three decay chains, each consisting of an implanted heavy atom and six subsequent alpha decays, correlated in time and position. A fourth event involving a number of "escape" alpha-particles (depositing only part of their energy in the detector) was reported too [2,3]. Based upon the above three chains, and a revised estimate of the beam dose in the 1999 experiments, a cross-section of 7^{+9}_{-3} pb was deduced for the synthesis of element 118 at a projectile energy (center of target, lab system) of 449 MeV. A new calibration of the magnetic rigidities ($B\rho$) of the Berkeley Gas-Filled Separator (BGS) indicates that the reported element 118 compound-nucleus evaporation residues (EVRs) recoiling from the target would have had a $B\rho$ of 2.00 Tm in the 130 Pa He gas of the separator. Attempts to reproduce this result by other groups [4–6] were unsuccessful.

Subsequently, the claim to synthesis of element 118 using the ^{208}Pb(^{86}Kr,n) reaction has been retracted [7]. That retraction was based upon the absence of the reported [1–3] chains in a re-analysis of the binary data on the original 1999 data tapes. An investigation into this matter has concluded that there was scientific misconduct and data fabrication by one individual [8]. GSI has also reported similar spurious data [9]. Despite the retraction of this claim, the current work is important in establishing definitive upper limits on the production of element 118 in the ^{208}Pb(^{86}Kr,n) reaction.

Motivated in part by the erroneous report [1], there have been a number of papers [10–22] predicting the structure and decay properties of element 118 and its daughters. Should element 118 be synthesized, it will be interesting to compare these predictions with the observations. In a similar vein, there have been a number of papers [23–37] dealing with the synthesis of element 118 and the reported production cross-section, which was unexpectedly large. Special mention should be made of the work of Smolańczuk [23,30] which prompted the experimental measurement [1]. Smolańczuk originally estimated [23] a production cross-section of 670 pb for the ^{208}Pb(^{86}Kr,n) reaction, an estimate that was later revised [30] to 5.9 pb. Other predictions [32–34] for the evaporation residue production cross-section for the reaction of 449 MeV ^{86}Kr

[a] e-mail: KEGregorich@lbl.gov

Table 1. "One-event" upper-limit cross-sections for formation of element 118 in the ^{208}Pb(^{86}Kr,n) reaction.

E^*(MeV)	Dose	Separator-$B\rho$	One-event upper limit (pb)	Reference
13.2	1.1×10^{18}	BGS-2.00 Tm	0.9	this work
13.2	1.5×10^{18}	BGS-2.12 Tm	0.6	this work
13.2	1.1×10^{18}	GANIL-LISE velocity filter	2.1	[5]
13.2	2.0×10^{18}	GARIS-2.1 Tm	0.6	[6]
13.2	2.9×10^{18}	GSI-SHIP velocity filter	0.5	[4]
15.5	0.4×10^{18}	GSI-SHIP velocity filter	3.6	[4]

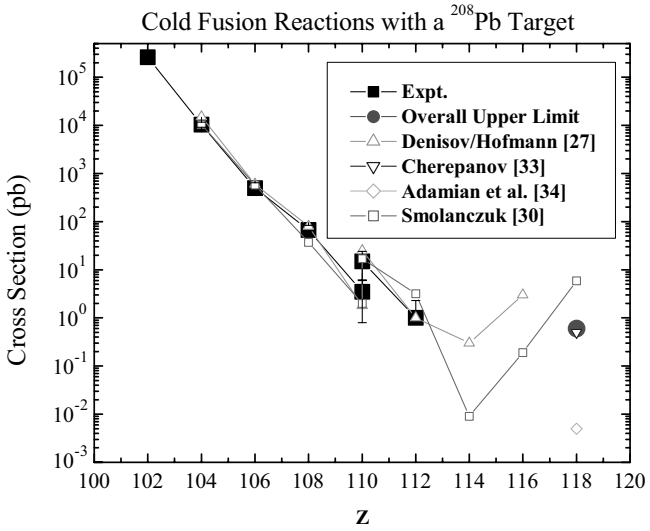

Fig. 1. The predicted and observed cross-sections for the synthesis of heavy nuclei for cold-fusion reactions involving a ^{208}Pb target.

with ^{208}Pb range from 0.005 to 2 pb. These predicted cross-sections are generally larger than expected from a simple logarithmic extrapolation of the trend of cross-sections for reactions of the type ^{208}Pb(X,n) [4] (fig. 1). Similar predictions of a non-exponential decrease in cold-fusion cross-sections for reactions leading to elements 116 and lighter elements have been made [27]. The physical effect behind this trend was pointed out by Myers and Swiatecki [25,28] as due to a sinking of the Coulomb barrier below the bombarding energy for symmetric target-projectile combinations, thus "unshielding" the saddle point. As pointed out by Siwek-Wilczynska and Wilczynski [31], the system in these cases must still evolve from the dinuclear composite system into the compound nucleus. Thus, even the establishment of upper limits for the ^{208}Pb(^{86}Kr,n) cross-section may contribute to our understanding of the large-scale collective motion in very heavy nuclei.

Besides the work presented herein, three recent attempts to reproduce the observations of [1] have been reported [4–6]. We summarize these attempts in table 1 in terms of the beam energy used, the particle dose and the observed upper-limit cross-section. All upper-limit cross-sections are reported as "one-event upper limits", *i.e.*, the cross-section that would have been reported had one event been observed with the given particle dose, target thickness, separator efficiency, etc. In the case of the data in [5], a separator efficiency of 50% [38] was used to calculate the cross-section. All excitation energies were calculated from [26].

2 2001 experimental setup

The reaction ^{208}Pb(^{86}Kr,n) was studied at the 88-Inch Cyclotron of the Lawrence Berkeley National Laboratory, using the Berkeley Gas-Filled Separator [39]. The experimental apparatus was a modified, improved version of the apparatus used in [1], including improved detectors and data acquisition systems, continuous monitoring of the separator gas purity, and a better monitoring of the ^{86}Kr beam intensity. A ^{86}Kr^{19+} beam was accelerated to 457 MeV with an average current of $\sim 1.3 \times 10^{12}$ ions/s. The beam went through the 40 μg/cm^2 carbon entrance window of the separator before passing through the ^{208}Pb target placed 0.5 cm downstream from the window. The targets were 470 μg/cm^2 thick (sandwiched between 40 μg/cm^2 C on the upstream side and 10 μg/cm^2 C on the downstream side). Nine of the arc-shaped targets were mounted on a 35 cm wheel that was rotated at 300 rpm. The beam energy in the target was 453–445 MeV [40], encompassing the in-target energies used in [1]. The reproducibility of beam energies from the 88-Inch Cyclotron was determined by measuring the beam energy spectrum in a Si p-i-n diode for 7 different ^{48}Ca beam energies between 203 and 219 MeV. Deviations from the expected linear relationship between energy deposit in the p-i-n diode and the square of the cyclotron frequency gave a standard deviation of 0.2% (FWHM = 0.5%) for the beam energy. The beam intensity in the BGS was monitored by two silicon p-i-n detectors (mounted at $\pm$27 degrees with respect to the incident beam) that detected elastically scattered beam particles from the target. Attenuating screens were installed in front of these detectors to reduce the number of particles reaching them (and any subsequent radiation damage to the detector). These detectors, the ^{208}Pb targets and the separator entrance window were replaced periodically during the run which lasted three weeks.

The EVRs ($E \sim 131$ MeV) were separated spatially in flight from beam particles and transfer reaction products by their differing magnetic rigidities in the gas-filled separator. The separator was filled with helium gas at a pressure of 130 Pa. The expected magnetic rigidities of

131 MeV ^{293}118 EVRs were estimated using the data of Ghiorso *et al.* [41]. These estimates were 2.00 Tm from extrapolation of the data in their fig. 3, and 2.10 Tm from their semi-empirical formula for EVR charge. In the current experiments, two settings of the magnetic fields of the separator were used, 2.00 Tm and 2.12 Tm. These settings differ by 6%, the width in magnetic rigidity of the focal-plane detector. The efficiency of the separator for transport and implantation of $Z = 118$ EVRs was estimated to be $\sim$ 79% using a Monte Carlo simulation described below.

The detector setup at the focal plane of the separator consisted of a parallel plate avalanche counter (PPAC) [42] placed $\sim$ 29 cm upstream of a Si-strip detector. The 10 cm $\times$ 10 cm PPAC registered time, energy loss, and x, y position of the particles passing through it. It has a thickness equivalent to $\sim$ 0.6 mg/cm^2 of carbon. The time of flight of the EVRs between the PPAC and the Si-strip detector was also recorded. The PPAC was used to distinguish between events arising from beam-related particles being implanted into the Si-strip detector, and those arising from the decay of previously implanted atoms. During these experiments, the PPAC efficiency for detecting beam-related particles depositing between 8 and 14 MeV in the Si-strip detector was 97.5–99.5%.

The 300 μm thick passivated ion-implanted silicon-strip detector had 32 vertical strips and an active area of 116 mm $\times$ 58 mm. The strips were position sensitive in the vertical (58 mm) direction. The sources used for position and energy calibrations are summarized in table 2. The energy resolution of the focal-plane detector was measured during the ^{86}Kr + ^{208}Pb experiments using the 7.45 MeV ^{211}Po background peak. The energy resolution was 42 keV (FWHM). The differences in measured positions for the ^{252}No - ^{248}Fm full energy α-α correlations in the ^{48}Ca + ^{206}Pb study had a Gaussian distribution with a FWHM of 0.52 mm ($\sigma = 0.22$ mm). The measured position resolution for full-energy alpha-particles correlated to "escape" alpha-particles (which deposited only 0.5–3.0 MeV in the detector) was $\sim$ 1.2 mm (FWHM). A second silicon-strip "punch-through" detector was installed behind this detector to reject particles passing through the primary detector. A "top" and a "bottom" detector were installed upstream of the focal-plane detector to detect escaping alpha-particles and fission fragments. The focal-plane detector combined with these "top" and "bottom" detectors had an estimated efficiency of 75% for the detection of full-energy 11 MeV α-particles following implantation of a ^{293}118 nucleus.

Any event with $E > 0.5$ MeV in the focal-plane Si-strip detector triggered the data acquisition. Data were recorded in list mode, and included the time of the trigger, the position and energy signals from the PPAC and the Si-strip detectors, and energy signals from the "top", "bottom" and "punch-through" detectors. With the use of buffering ADCs and scalers, the minimum time between successive events was 15 μs.

The energies of the ^{293}118 EVRs, after passing through the PPAC, were estimated to be $\sim$73 MeV by extrapolation of heavy-ion stopping powers, calculated with SRIM2000 [40]. The ^{293}118 implantation pulse height in the Si-strip detector was estimated to be 24–48 MeV after applying the pulse-height defect determined for Rn EVRs from the 365 MeV ^{86}Kr + ^{120}Sn reaction.

With a beam current of 1.3×10^{12} ^{86}Kr ions striking the target, the average total counting rates ($E > 0.5$ MeV) in the focal-plane detector were $\sim$ 40/s and $\sim$ 10/s at $B\rho$ settings of 2.00 and 2.12 Tm, respectively. The average rate of "alpha-particles" (8–14 MeV with no PPAC signal) was $\sim$ 0.2/s.

3 Results

At separator magnet settings corresponding to EVR magnetic rigidities of 2.00 and 2.12 Tm, the projectile doses were 1.1×10^{18} and 1.5×10^{18}, respectively. No event chains similar to those reported in [1] or as predicted [10–21] for the decay of ^{293}118 were observed. Two independent searches were performed for superheavy element (SHE) decay sequences. In the first, a search routine in the GOOSY [43] environment was used to search for events similar to those reported in [1], *i.e.*, a search was made for events in which two alpha-particle decays were detected in the focal-plane detector within 30 ms and with positions differing by < 1.5 mm. The energies of the alpha-particles had to be greater than 10 MeV and they had to be unrelated to beam events (no PPAC signal). No such α-α correlations were found.

A second, less restrictive search was made for EVRs ($>$ 20 MeV with a PPAC signal) followed by alpha decays (8-14 MeV in the focal-plane Si-strip detector, no PPAC signal) correlated in position ($\pm$2 mm, same strip) and time (within 10 s). For this search, one detector strip on the low-$B\rho$ edge of the detector and three strips on the high-$B\rho$ edge of the detector were excluded because they detected relatively high rates of scattered beam particles with trajectories bypassing the PPAC. Two potential EVR-α-α chains were identified. Based on the singles rates for alpha-like events and EVRs, the expected number of random EVR-α-α chains is $\sim$ 4. Both of the observed EVR-α-α chains had large differences in the vertical positions for the parent and daughter alpha-particles, $|\Delta p| \geq 0.78\,\mathrm{mm} = 3.5\sigma$. Thus, we conclude that there are no valid EVR-α-α correlations in the data set from this experiment.

One must also consider the possibility that SHEs decay by spontaneous fission (SF). Spontaneous fission events in which one fragment was detected in the focal-plane detector ($E > 90$ MeV, no PPAC signal) can be confused with scattered ^{86}Kr beam particles not vetoed by the PPAC signal. Therefore, we excluded, from the analysis, three strips on the low-$B\rho$ edge of the detector and four strips on the high-$B\rho$ edge of the detector to discriminate against these scattered beam particles. We observed no single fission fragment signals during the run using these gating conditions, *i.e.*, no EVR-SF events.

There were no correlation chains containing at least EVR-α-α or EVR-SF with additional full-energy

Table 2. BGS energy calibration points.

Calibration reaction	Nuclide	Energy (MeV)	Nuclide	Energy (MeV)
External source	^{148}Gd	3.183	^{239}Pu	5.157
	^{241}Am	5.486	^{244}Cm	5.805
365 MeV ^{86}Kr + ^{120}Sn	^{204}Rn	6.417	^{203}Rn	6.497, 6.547
218 MeV ^{48}Ca + ^{208}Pb	^{254}No	8.10	^{250}Fm	7.43
218 MeV ^{48}Ca + ^{206}Pb	^{252}No	SF	^{252}No	8.42
	^{248}Fm	7.87	^{244}Cf	7.209

alpha-particles (8–14 MeV with no PPAC signal) or escape alpha-particles (with energy deposited in the focal-plane detector > 0.5 MeV and no PPAC signal).

The implantation depth in the Si-strip detector for the ^{293}118 recoils ($E \sim 73$ MeV after passing through the PPAC) was extrapolated from heavy-ion ranges calculated with SRIM2000 [40], and is estimated to be 7 μm. From this depth, the efficiency for detecting full energy for isotropically emitted 8–14 MeV alpha-particles is 55%. The expected decay sequence [22,1] following implantation of a ^{293}118 EVR consists of 6 α-particles emitted sequentially within the first 10 seconds after implantation. Using the 55% α-particle efficiency, ε, together with a binomial series for the probability P of observing at least n members of an N-member chain,

$$P = \sum_{a=n}^{N} \frac{N!}{a!(N-a)!} \varepsilon^a (1-\varepsilon)^{N-a}\,, \qquad (1)$$

the probability for detecting at least two full-energy α-particles from a sequence of six is 93%. Such a binomial treatment can be used to calculate the efficiency for detection of other postulated decay chains. Assuming a 100% event chain detection efficiency results in "one-event" upper-limit cross-sections of 0.9 pb and 0.6 pb for $B\rho$ settings of 2.00 and 2.12 Tm, respectively. These cross-section limits assume detection of one event, whereas none were observed, and a constant production cross-section throughout the target thickness.

4 Discussion

4.1 Cross-section calculation

The standard cross-section calculation assumes a constant cross-section, $\sigma_{\rm const}$, for all beam energies within the target. The number of events observed, $n_{\rm obs}$, is given by

$$n_{\rm obs} = \phi t \cdot N_t \cdot \sigma_{\rm const} \cdot \varepsilon\,, \qquad (2)$$

where ϕt is the integrated beam current, N_t is the areal density of target atoms, and ε is the experimental efficiency. This formalism was used in [4-6] for the cross-section limits quoted in those works and used above in table 1 and related discussion. However, in the case of the ^{208}Pb(^{86}Kr,n)^{293}118 reaction, the excitation function is expected to be narrow and the energy loss of the beam in traversing the target material is relatively large ($\Delta E \sim 8$ MeV) [40], so the assumption of a constant cross-section for all beam energies within the target does not hold. For the purpose of an improved determination of cross-section limits in this experiment, a Gaussian excitation function, $\sigma(E)$, with a full-width at half-maximum (FWHM) of 5 MeV in the lab frame has been assumed:

$$\sigma(E) = \sigma_c \exp((E-c)^2/2s^2)\,, \qquad (3)$$

where σ_c is the cross-section at c, the centroid energy, E is the beam energy at the corresponding target depth, and s is the standard deviation of the Gaussian ($s = 2.12$ MeV for a 5 MeV FWHM). This results in the differential equation

$$\partial n_{\rm obs} = \phi t \cdot \frac{\partial N_t(E)}{\partial E} \cdot \sigma(E) \cdot \varepsilon(E) \cdot \partial E\,, \qquad (4)$$

where the separator efficiency, $\varepsilon(E)$, depends on the beam energy (depth in target). Since the areal number density of target atoms and the $\mathrm{d}E/\mathrm{d}x$ of the beam are nearly constant throughout the target, the areal number density of target atoms within a differential target thickness element, $\frac{\partial N_t(E)}{\partial E}$, is constant and equal to $N_t/\Delta E$, where ΔE is 8.0 MeV for the ^{86}Kr beam in the ^{208}Pb targets. Integrating over the energy range in the target, and solving for σ_c results in

$$\sigma_c = \frac{n_{\rm obs}}{\left[\phi t \cdot \frac{N_t}{\Delta E} \cdot \int_{E_i}^{E_f} \varepsilon(E) \exp\left[-\frac{(E-c)^2}{2s^2}\right] \mathrm{d}E\right]}\,, \qquad (5)$$

where E_i and E_f are the beam energies at the upstream and downstream limits of the target. For our experiment, assuming that the centroid of the excitation function corresponds to the center of the target and that the efficiency is constant throughout the target, $\sigma_c/\sigma_{\rm const} = 1.6$, and thus the cross-section limits presented below are larger than those calculated in the traditional way by this factor.

4.2 BGS Efficiency simulation

The efficiency of the BGS is limited by the initial position, energy and angular distributions of recoils exiting the target, and by transmission of these recoils through the BGS under the influence of the magnetic fields, and energy loss, multiple scattering and charge exchange in the He fill gas.

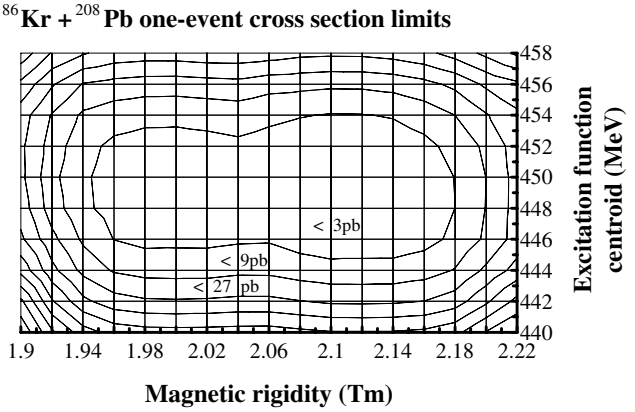

Fig. 2. The one-event upper-limit cross-sections measured in this work as a function of the assumed excitation function centroid energy and recoil magnetic rigidity.

All of these effects, together with the effects of the estimated angular and energy distributions of the ^{86}Kr beam entering the BGS were calculated with a Monte Carlo simulation. In this simulation, the initial ^{86}Kr beam energies and directions were chosen from an assumed Gaussian energy distribution (with a centroid of 457 MeV —chosen to put c at the center of the target, and a 0.3% FWHM— a typical beam energy width from the 88-Inch Cyclotron) and Gaussian angular (FWHM = 0.9° —typical for the beamline leading to the BGS) distributions. The beam energy was corrected for energy loss in the carbon entrance window and target backings. Points were randomly chosen from the assumed Gaussian excitation function (c = 449 MeV, s = 2.12 MeV), and if they were within the energy range subtended by the target (thickness = 0.47 mg/cm^2, dE/dx = 17 MeV/(mg/cm^2)), the depth of interaction in the target was calculated, and a simulation of the trajectory of an EVR was initiated. The initial energy and angle of the EVR were corrected for the effect of isotropic evaporation of a single neutron. Energy loss and angular scattering in the remaining target material was calculated for each EVR using SRIM2000 [40]. After exiting the target, the trajectories through the BGS were simulated, including the effects of the magnetic fields, charge exchange in the gas, scattering in the gas, and energy loss in the gas. By comparing the number of EVRs reaching the focal-plane detector in the simulation with the initial number of ^{86}Kr beam particles, the effects of the fraction of the excitation function contained in the target and the BGS efficiency as a function of target depth were accounted for. The "average" separator transport efficiency for the EVRs produced in this reaction was calculated to be 79%.

4.3 Improved ^{293}118 cross-section upper limits

Since neither the centroid of the element 118 excitation function nor the magnetic rigidity of the Z = 118 EVRs are known, numerical simulations of the BGS efficiency were run using several different choices for the excitation function centroid energy and average EVR magnetic rigidity. These simulations gave a set of experimental sensitivities as a function of the assumed excitation function centroid, and of the assumed magnetic rigidity. The results from two bombardments, the first with 1.1×10^{18} ^{86}Kr ions at a BGS magnetic rigidity ($B\rho$) of 2.00 Tm and the second with 1.5×10^{18} Kr ions and $B\rho$ = 2.12 Tm were combined. The one-event cross-section limits (assuming observation of one element 118 chain where zero events were observed) as a function of assumed σ_c and $B\rho$ are presented in fig. 2. The cross-section limits reached were as low as 1.1 pb, and a limit of less than 4.5 pb was reached for compound-nucleus excitation energies from 10.0–16.8 MeV (444.5 $<$ $E_{\rm lab}$ (MeV) $<$ 454.0), covering magnetic rigidities for the recoiling products from 1.94–2.18 Tm.

5 Summary

Several experiments have led to one-event cross-section upper limits near 0.6 pb for the 449 MeV ^{208}Pb(^{86}Kr,n)^{293}118 reaction (table 1). In fig. 1, we compare this 0.6 pb limit with various theoretical predictions [27,30,33,34] for the production of ^{293}118 in the reaction of 449 MeV ^{86}Kr with ^{208}Pb. This limit is below some of the predicted values. Combination of sets of upper-limit cross-sections from table 1 results in an upper-limit cross-section of $\sim$ 0.2 pb, placing more stringent limitations on the validity of some of the models. The most pessimistic estimate [34] of the evaporation residue cross-section assumes the probability of forming a true compound nucleus, after capture of the projectile, decreases by approximately four orders of magnitude in going from ^{70}Zn + ^{208}Pb to ^{86}Kr + ^{208}Pb. This decrease may counteract any fusion enhancement due to a lowering of the Coulomb barrier relative to the energy of the fused system in the latter reaction. Observation of the production of element 118 in the ^{208}Pb(^{86}Kr,n) reaction will require sensitivity to cross-sections smaller than $\sim$ 0.2 pb.

We gratefully acknowledge the operations staff of the 88-Inch Cyclotron and ion source person Daniela Wutte for providing intense, steady beams of ^{86}Kr. We thank Larry Phair for his help in the re-analysis of the 1999 data. We thank Patrick Gamman and Helmut Folger for providing the carbon entrance windows, and the lead targets. Financial support was provided by the Office of High Energy and Nuclear Physics, Nuclear Physics Division of the U.S. Department of Energy, under contract DE-AC03-76SF00098 and grant DE-FG06-97ER41026, the Norwegian Research Council (project No. 138507/410) and The Swedish Foundation for International Cooperation in Research and Higher Education.

References

1. V. Ninov *et al.*, Phys. Rev. Lett. **83**, 1104 (1999).
2. K.E. Gregorich, V. Ninov, in *Origin of the Elements in the Solar System*, edited by O. Manuel (Kluwer, New York, 2000) pp. 21-34.

3. K.E. Gregorich, V. Ninov, J. Nucl. Radiochem. Sci. **1**, 1 (2000).
4. S. Hofmann, G. Munzenberg, Rev. Mod. Phys. **72**, 733 (2000).
5. C. Stodel *et al.*, AIP Conf. Proc. **561**, 344 (2001).
6. K. Morimoto, AIP Conf. Proc. **561**, 354 (2001).
7. V. Ninov *et al.*, Phys. Rev. Lett. **89**, 039901 (2002).
8. M. Gilchriese, A. Sessler, G. Trilling, R. Vogt, Lawrence Berkeley National Laboratory Report, LBNL-51773, (2002).
9. S. Hofmann *et al.*, Eur. Phys. J. A **14**, 147 (2002).
10. S. Ćwiok, W. Nazarewicz, P.H. Heenen, Phys. Rev. Lett. **83**, 1108 (1999).
11. A. Mamdouh, J.M. Pearson, M. Rayet, F. Tondeur, Nucl. Phys. A **679**, 337 (2001).
12. M. Bender, *Proceedings of the International Conference on Fusion Dynamics at the Extremes, Dubna, Russia, May 25-27, 2000*, edited by Yu.Ts. Oganessian, V.I. Zagrabev (World Scientific, Singapore, 2001) pp. 51-64.
13. M. Bender, Phys. Rev. C **61**, 031302 (2000).
14. A.T. Kruppa, M. Bender, W. Nazarewicz, P.-G. Reinhard, T. Vertse, S. Cwiok, Phys. Rev. C **61**, 034313 (2000).
15. J. Meng, N. Takigawa, Phys. Rev. C **61**, 064319 (2000).
16. Z. Ren, H. Toki, Nucl. Phys. A **689**, 691 (2000).
17. M. Bender, W. Nazarewicz, P.-G. Reinhard, Phys. Lett. B **15**, 42 (2001).
18. Ch. Beckmann, P. Papazoglu, D. Zschiesche, S. Schramm, H. Stocker, W. Greiner, Phys. Rev. C **65**, 024301 (2002).
19. H. Koura, AIP Conf. Proc. **561**, 388 (2001).
20. P.-G. Reinhard, M. Bender, T. Burvenich, T. Cornelius, P. Fleischer, J.A. Maruhn, AIP Conf. Proc. **561**, 377 (2001).
21. G. Royer, J. Phys. G. **26**, 1149 (2000).
22. R. Smolańczuk, Phys. Rev. C **56**, 812 (1997).
23. R. Smolańczuk, Phys. Rev. C **59**, 2634 (1999).
24. R. Smolańczuk, Phys. Rev. Lett. **83**, 4705 (1999).
25. W.D. Myers, W.J. Swiatecki, Acta Phys. Pol. B **32**, 1033 (2001).
26. R. Smolańczuk, Phys. Rev. C **61**, 011601(1999).
27. V.Yu. Denisov, S, Hofmann, Phys. Rev. C **61**, 034606 (2000).
28. W.D. Myers, W.J. Swiatecki, Phys. Rev. C **62**, 044610 (2000).
29. G.G. Adamian, N.V. Antonenko, S.P. Ivanova, W. Scheid, Phys. Rev. C **62**, 064303 (2000).
30. R. Smolańczuk, Phys. Rev. C **63**, 044607 (2001).
31. K. Siwek-Wilczynska, J. Wilczynski, Phys. Rev. C **64**, 024611 (2001).
32. V. Yu. Denisov, AIP Conf. Proc. **561**, 433 (2001).
33. E. Cherepanov, Pramana **53**, 619 (1999).
34. G.G. Adamian, N.V. Antonenko, A. Diaz-Torres, W. Scheid, Yu.M. Tchuvil'sky, AIP Conf. Proc. **561**, 421 (2001).
35. J. Giardina *et al.*, Izv. Akad. Nauk, Ser. Fiz. **64**, 862 (2000).
36. R.K. Gupta, M. Balasubramaniam, G.Munzenberg, W. Greiner, W. Scheid, J. Phys. G **27**, 867 (2001).
37. I. Muntian, Z. Patyk, A. Sobiczewski, Acta Phys. Pol. B **32**, 691 (2000).
38. C. Stodel, private communication.
39. V. Ninov, K.E. Gregorich, *ENAM98*, edited by B.M. Sherrill, D.J. Morrissey, C.N. Davids, AIP Conf. Proc. **455**, 704 (1999).
40. J.F. Ziegler, J.P. Biersack, U. Littmark, *The Stopping and Range of Ions in Solids* (Pergamon, New York, 1985); see also `http://www.srim.org`.
41. A. Ghiorso, S. Yashita, M.E. Leino, L. Frank, J. Kalnins, P. Armbruster, J.-P. Dufour, P.K. Lemmertz, Nucl. Instrum. Methods A **269**, 192 (1988).
42. D. Swan, J. Yurkon, D.J. Morrissey, Nucl. Instrum. Methods A **348**, 314 (1994).
43. See `http://www-gsi-vms.gsi.de/anal/home.html`.